14A.6 EFFECTS OF SURFACE EXCHANGE COEFFICIENTS ON THE INTENSITY AND STRUCTURE OF AXISYMMETRIC HURRICANES

Tristan J. Shepherd*, Kevin J.E. Walsh
University of Melbourne, Melbourne, Australia
Jeffrey D. Kepert
Centre for Australian Climate and Weather Research, Melbourne, Australia

1. INTRODUCTION

Recent advances in the subject of hurricane maximum potential intensity (MPI) (e.g. Bryan 2012) have indicated the ratio of enthalpy (C_k) to momentum (C_d) has less effect on maximum wind speed than the MPI theory suggested by Emanuel (1995) (hereafter E95). Emanuel's theory suggests a relationship between the C_k/C_d ratio and the maximum tangential velocity (V_{max}), where $V_{max} \sim (Ck/Cd)^{\frac{1}{2}}$. It has been shown by Rotunno and Bryan (2009) and Bryan (2012) (hereafter B12), however, that this relation for V_{max} is a reasonable approximation only for low values of the horizontal mixing length, with a lower exponent applying as this length increases.

Through a series of axisymmetric simulations we examine why this functional dependence might not be accurate. We propose that this conflict between the model simulations and the theory results from structural differences between storms when either C_k or C_d is varied, but C_k/C_d held constant. B12 showed V_{max} does not change much in these circumstances, but we find that the radius of maximum winds (RMW) and the boundary-layer flow are sensitive.

2. METHODS

Hurricanes were simulated for a range of enthalpy and drag coefficients using the axisymmetric model CM1. In the interests of consistency, we use the same model settings as described by B12, which is setup B res 2. For this setup, the model was initialized with the moist tropical sounding of Dunion (2011) with an SST of 29 °C. The Morrison et al. (2009) microphysics scheme was used. The total number of vertical levels was 123, with variable vertical grid spacing with height above 7 km, below which the grid spacing was 250 m. The horizontal grid spacing out to 64 km is 1 km, at which point the spacing gradually increases out to 15 km at the domain edge (1500 km).

Nine simulations tested the E95 MPI theory, with C_k/C_d ratios of 0.5, 1.0 and 2.0 for constant values of C_d of 1.5×10^{-3}, 2×10^{-3} and 3×10^{-3} (Table 1). All simulations used a horizontal turbulence length scale of l_h = 1000 m and vertical length scale of l_v = 50 m. The simulation length in each case was 12 days, except experiments 1 and 2, which were for 24 days.

Results of structure presented herein were averaged over the final 6 days of the simulation. We calculate V_{max} using a 2-day running mean and apply a conversion factor to calculate the 10 m wind speed.

Table 1. List of experiments and associated values.

Experiment #	C_k/C_d ratio	C_d value	C_k value
1	N/A	Large & Pond	1.5×10^{-3}
2	N/A	Capped at 1.3×10^{-3}	1.5×10^{-3}
3	0.5	1.5×10^{-3}	0.75×10^{-3}
4	0.5	2×10^{-3}	1×10^{-3}
5	0.5	3×10^{-3}	1.5×10^{-3}
6	1	1.5×10^{-3}	1.5×10^{-3}
7	1	2×10^{-3}	2×10^{-3}
8	1	3×10^{-3}	3×10^{-3}
9	2	1.5×10^{-3}	3×10^{-3}
10	2	2×10^{-3}	4×10^{-3}
11	2	3×10^{-3}	6×10^{-3}

3. RESULTS

The results presented here agree with those of B12, that the sensitivity to C_k/C_d for model produced V_{max} is less than stated by the Emanuel (1995) theory. Figure 1 shows C_k/C_d ratio against V_{max} for the present study and B12. The slope is much less than expected from Emanuel (1995). Here, we find $V_{max} \sim (Ck/Cd)^{0.215}$ for l_v = 50 m, l_h = 1000 m and using a slightly higher C_k than in B12. B12 found $V_{max} \sim (Ck/Cd)^{0.127}$ using those settings with $C_k = 1.2 \times 10^{-3}$.

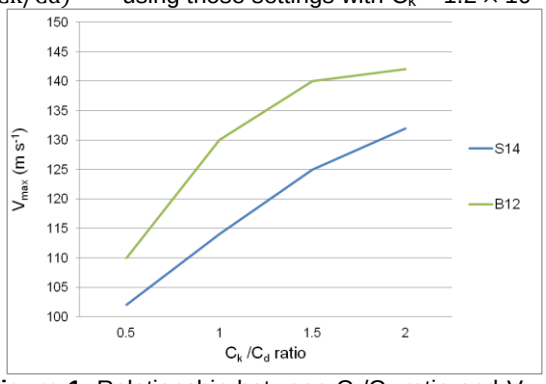

Figure 1. Relationship between C_k/C_d ratio and V_{max}, for B12 and the present MPI study (S14). Note the B12 values are from his Figure 3b and are for constant C_k of 1.2×10^{-3} and l_v = 50 m, l_h = 1000 m.

* *Corresponding author address*: Tristan J. Shepherd, Univ. of Melbourne, Sch. of Earth Sciences, VIC 3010, Australia; email: t.shepherd@student.unimelb.edu.au

A time series plot of experiments 3 and 5 (Figure 2) where C_d and C_k are increased in experiment 5, shows, as expected, an increase in enthalpy despite an increase in drag, produces a more intense storm. Note the spinup time required to generate a steady state, but that some variability can occur during the life cycle. This has been noted by Brown and Hakim (2013).

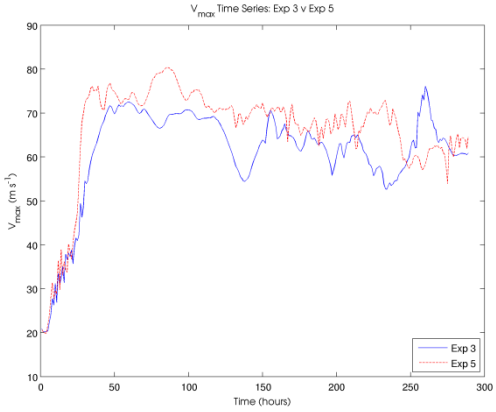

Figure 2. Time series of V_{max} (converted to 10 m wind speed values) for $C_k/C_d = 0.5$. Experiment 3 has $C_d = 1.5 \times 10^{-3}$ and $C_k = 0.75 \times 10^{-3}$. Experiment 5 has $C_d = 3 \times 10^{-3}$ and $C_k = 1.5 \times 10^{-3}$.

A structural comparison of experiments 3 and 5 (Figure 3), shows the change in the size and positioning of the RMW. The radius to which the 25 m s^{-1} winds extend also changed. These changes were systematically seen across all experiments (not shown).

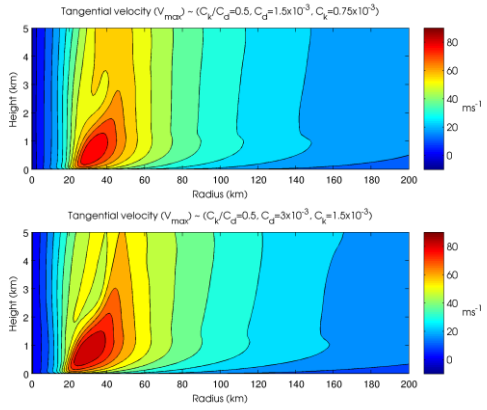

Figure 3. 6-day averaged V_{max} for Experiment 3 (top) and experiment 5 (bottom). Note the size increase of the RMW and the movement of the RMW closer to the storm center in experiment 5.

In order to explain some of the reasons why these changes occur, and, in particular, why the RMW shifts, difference plots of angular momentum and V_{max} (Figure 4) are shown. Here, the case of $C_d = 1.5 \times 10^{-3}$ / $C_k = 0.75 \times 10^{-3}$ (experiment 3) is subtracted from the increased C_d and C_k experiment (where $C_d = 3 \times 10^{-3}$ / $C_k = 1.5 \times 10^{-3}$). There is more drag at both lower and higher wind speeds in experiment 5. As a result, there is less angular momentum in the lower wind speed regions of the boundary-layer at larger radius. We would expect the higher wind speed regions of the eyewall to behave similarly, but the increase of C_k means the intensity of the storm offsets the C_d increase and thus more angular momentum is observed in the eyewall. The plot of V_{max} confirms the increased intensity in the eyewall, but at larger radius the winds are slightly weaker.

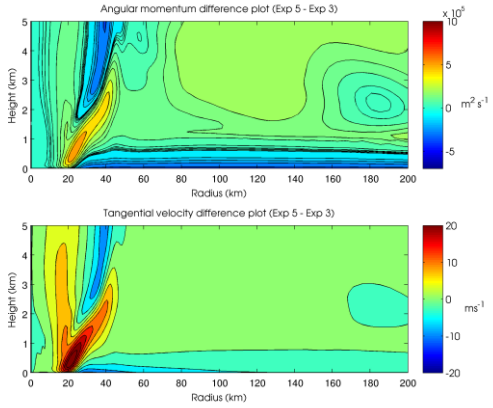

Figure 4. Difference plot of angular momentum (top) and V_{max} (bottom) for experiment 3 and experiment 5. Experiment 3 has $C_k/C_d = 0.5$ with $C_d = 1.5 \times 10^{-3}$ and C_k 0.75×10^{-3}. Experiment 5 has $C_k/C_d = 0.5$ with $C_d = 3 \times 10^{-3}$ and $C_k = 1.5 \times 10^{-3}$.

A further plot (Figure 5) shows the difference between two experiments with the same C_k, but different C_d. For this difference plot, the case of less drag (experiment 6) is subtracted from the case with more drag (experiment 5). The top panel in Figure 5 shows there is less angular momentum in experiment 5 because there is more drag at all wind speeds. The only area where angular momentum is greater for experiment 5 than in experiment 6 is in the boundary-layer in the eyewall. Given there is more drag at high wind speed in experiment 5, the opposite would be expected (as is seen at larger radii). Since the differences are larger near the surface, it is evident that boundary-layer dynamics play an important role, consistent with earlier studies that have shown a contraction of the RMW at landfall (e.g. Kepert 2002).

4. CONCLUSIONS

The results of axisymmetric simulations presented here agree with Bryan (2012) who showed for large values of horizontal mixing length that the C_k/C_d ratio and V_{max} relationship is weaker than suggested by Emanuel (1995). Further examination of the structure shows the position of the RMW varies quite considerably regardless of changes to the C_k/C_d ratio (i.e. the shift is observed for experiments with the same C_k but different C_d).

Initial analysis shows a redistribution of the angular momentum is one possible cause for this RMW shift, but further analysis, including the derivation of angular momentum budgets is required to determine the exact cause for why this change is seen. Understanding the cause of these structural changes may help with the development of an improved MPI theory.

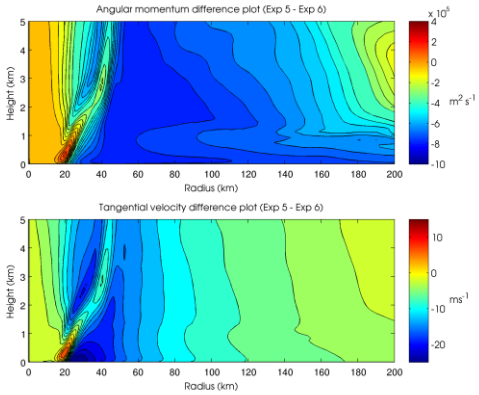

Figure 5. Difference plot of angular momentum (top) and V_{max} (bottom) for experiment 5 and experiment 6. Experiment 5 has $C_k/C_d = 0.5$ with $C_d = 3 \times 10^{-3}$ and C_k 1.5×10^{-3}. Experiment 6 has $C_k/C_d = 1$ with $C_d = 1.5 \times 10^{-3}$ and $C_k = 1.5 \times 10^{-3}$.

5. REFERENCES

Brown, B.R., and Hakim, G.J., 2013: Variability and predictability of a three-dimensional hurricane in statistical equilibrium. *J. Atmos. Sci.*, **70**, 1806-1820.

Bryan, G.H., 2012: Effects of surface exchange coefficients and turbulence length scales on the intensity and structure of numerically simulated hurricanes. *Mon. Wea. Rev.*, **140**, 1125-1143.

Dunion 2011, J.P., 2011: Rewriting the climatology of the tropical North Atlantic and Caribbean Sea atmosphere. *J. Climate*, **24**, 893-908.

Emanuel, K.A., 1995: Sensitivity of tropical cyclones to surface exchange coefficients and a revised steady-state model incorporating eye dynamics. *J. Atmos. Sci.*, **52**, 3969-3976.

Kepert, J., 2002: The impact of landfall on tropical cyclone boundary layer winds. Extended abstracts, *25th Conf. on Hurricanes and Tropical Meteorology*, San Diego, CA, Amer. Meteor. Soc., 29 April – 3 May, 335–336.

Morrison, H., Thompson, G., and Tatarskii, V., 2009: Impact of cloud microphysics on the development of trailing stratiform precipitation in a simulated squall line: Comparison of one- and two-moment schemes. *Mon. Wea. Rev.*, **137**, 991-1007.

Rotunno, R., and Bryan, G.H., 2009: The maximum intensity of tropical cyclones in axisymmetric numerical model simulations. *Mon. Wea. Rev.*, **137**, 1770-1789.